# Crystal Structure of the YcjX Stress Protein Reveals a Ras-Like GTP-Binding Protein

**Joshua T. Tsai[1], Nuri Sung[1], Jungsoon Lee[1], Changsoo Chang[2], Sukyeong Lee[1] and Francis T.F. Tsai[1,3,4]**

*1 - **Verna and Marrs McLean Department of Biochemistry and Molecular Biology,** Baylor College of Medicine, Houston, TX 77030, USA*
*2 - **Structural Biology Center,** Biosciences Division, Argonne National Laboratory, Argonne, IL 60439, USA*
*3 - **Department of Molecular and Cellular Biology,** Baylor College of Medicine, Houston, TX 77030, USA*
*4 - **Department of Molecular Virology and Microbiology,** Baylor College of Medicine, Houston, TX 77030, USA*

***Correspondence to Sukyeong Lee and Francis T.F. Tsai:**. Department of Biochemistry, Baylor College of Medicine, One Baylor Plaza, MS: BCM125, Houston, TX 77030, USA. slee@bcm.edu, ftsai@bcm.edu.*
https://doi.org/10.1016/j.jmb.2019.06.006
***Edited by M. Guss***

## Abstract

Stress proteins promote cell survival by monitoring protein homeostasis in cells and organelles. YcjX is a conserved protein of unknown function, which is highly upregulated in response to acute and chronic stress. Notably, heat shock induction of *ycjX* exceeded even levels observed for major stress-induced chaperones, including GroEL, ClpB, and HtpG, which use ATP as energy source. YcjX features a Walker-type nucleotide-binding domain indicating that YcjX might function as a molecular chaperone. Here, we present the first crystal structure of YcjX from *Shewanella oneidensis* solved at 1.9-Å resolution by SAD phasing. We show that YcjX is a GTP-binding protein that shares at its core the canonical alpha-beta domain of $p21^{ras}$ (Ras). However, unlike Ras, YcjX features several unique insertions, including an entirely α-helical domain not previously observed in Ras-like GTPases. We note that this helical domain is reminiscent of a similar domain in the Gα subunit of heterotrimeric G proteins, supporting a potential role for YcjX as a signal transducer of stress responses. To elucidate the mechanism of GTP hydrolysis, we determined crystal structures of YcjX bound to GDP and GDPCP, respectively, which crystallized in three different nucleotide switch conformations. Supported by targeted mutagenesis experiments, we show that YcjX utilizes a non-canonical switch 2′ motif not previously observed in Ras-like GTPases. Together, our structures provide atomic snapshots of YcjX in different functional states, illustrating the structural determinants for stress signaling.


## Introduction

The ability of cells to survive exposure to acute and chronic stress is essential to organismal health. To cope with different stress conditions, cells have evolved sophisticated surveillance mechanisms that control transcriptional responses and upregulate the expression of stress proteins to maintain proteostasis inside the cell [1]. Global reexamination of transcription patterns in *Escherichia coli* led to the identification of *ycjX* [2,3], whose mRNA level was induced greater than 39-fold in response to protein unfolding, exceeding even that of ATP-dependent molecular chaperones such as *groEL* (38-fold), *clpB* (37-fold), and *htpG* (34-fold) [4]. *YcjX* gene expression was also found to be highly upregulated under conditions of nitrogen starvation [5], indicating that YcjX is a general stress-response protein.

To inform on YcjX's biological function, we determined the high-resolution crystal structure of YcjX from *Shewanella oneidensis*, a facultative gram-negative bacterium known for its ability to reduce and absorb heavy metal ions. The structure was solved at 1.9-Å resolution by seleno-methionine (Se-Met) SAD phasing and revealed that YcjX shares at its core the GTP-binding domain of $p21^{ras}$ (Ras) but has several unique insertions, including a large α-helical domain not previously found in Ras-like GTPases. A hallmark of Ras GTPases and other

 

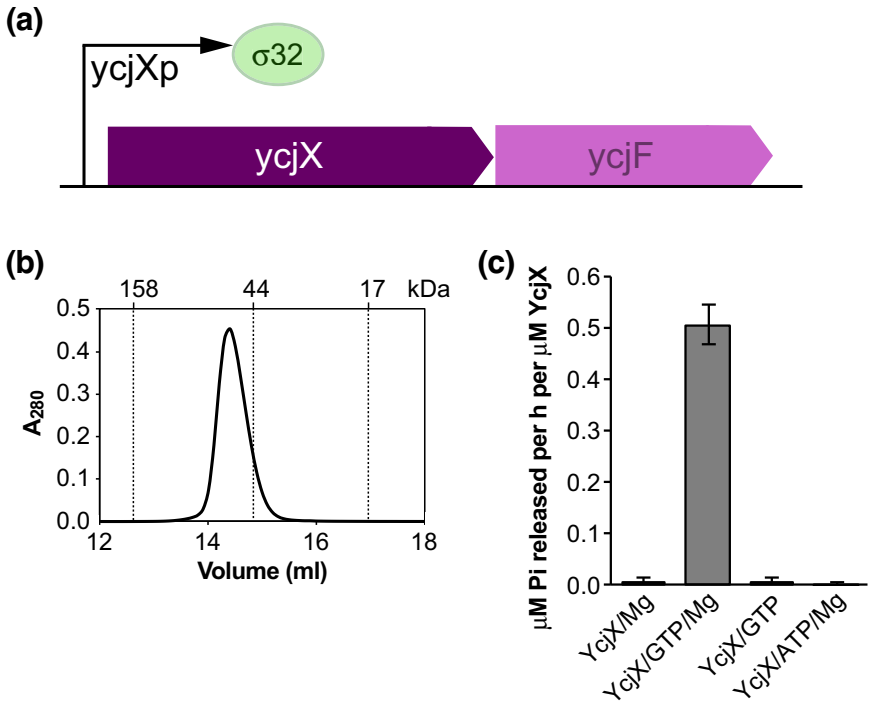


**Fig. 1.** YcjX is a monomeric GTP hydrolase. (a) Organization of the *ycjXF* gene cluster in gram-negative bacteria. (b) Analytical size-exclusion chromatogram shows that YcjX is a 58.3-kDa monomer in solution. (c) YcjX hydrolyzes GTP but not ATP and requires magnesium ions for catalysis. Averages of three independent measurements (n = 3) ± SD are shown.

guanine nucleotide-binding proteins (G proteins) is the conservation of sequence motifs, termed G1 to G5, which are essential for GTP binding, hydrolysis, or both. Structural comparison of both Ras-like GTPases and heterotrimeric G proteins in the tri- and di-phosphate states has confirmed that functionally important conformational changes during the GTP–GDP transition are confined to the conserved switch 1 (G2) and switch 2 (G3) motifs [6,7], which signal the nucleotide-bound status.

In the crystal, YcjX is bound to GDP that co-purified from the expression host. Surprisingly, closer inspection revealed that we had determined two different GDP-bound structures (GDP-Form I and GDP-Form II), which differed only in their nucleotide switch conformation. In addition to the inactive GDP-bound states, we also present the 2.2-Å resolution crystal structure of YcjX bound to GDPCP that mimics the GTP-bound state. Remarkably, our structures together with targeted mutagenesis experiments revealed that in addition to the conserved switch 1 and switch 2 motifs, YcjX utilizes a novel switch 2′ motif not previously observed in any other G protein. We propose that the three YcjX conformations represent snapshots of different functional states that together provide the structural basis for signal transduction.

## Results

### YcjX is a conserved stress protein in gram-negative bacteria

Transcription of the *ycjX* gene is under control of the $\sigma^{32}$ regulon that regulates the expression of several stress proteins (Fig. 1a), including stress-induced chaperones [8] and regulators of protein translation [9]. InterPro [10] classifies YcjX as a member of the PIRSF019381 superfamily that is ubiquitously found in gram-negative proteobacteria but is largely absent from gram-positive bacteria. YcjX consists of ~485 amino acids comprising the DUF463 domain of unknown function and features a canonical Walker A sequence motif [11], classifying YcjX as a phosphate-binding (P)-loop-containing nucleoside triphosphate hydrolase. Interestingly, the *ycjX* gene is always found upstream of *ycjF*, which codes for an integral membrane protein specifically expressed during bacterial septicemia [12]. Furthermore, it was noted that the *ycjXF* pair is frequently located adjacent to the *psp* operon, which contains genes that code for components of the phage-shock-protein (Psp) stress response [13,14]. In *E. coli*, the Psp stress response system is responsible for repairing damage to the inner

**Table 1.** Data collection, phasing, and refinement statistics

| Data collection | YcjX $_{F187L/D218G}$ GDP (Se-Met) | YcjX $_{F187L/D218G}$ GDP: Form I | YcjX $_{F187L/D218G}$ GDP: Form II | YcjX GDPCP |
|---|---|---|---|---|
| Space group | $P2_12_12_1$ | $P2_12_12_1$ | $P2_12_12_1$ | $P2_12_12_1$ |
| Cell dimensions | | | | |
| *a*, *b*, *c* (Å) | 62.54, 130.19, 140.26 | 59.31, 133.94, 144.62 | 59.39, 134.10, 145.02 | 59.47, 128.26, 148.06 |
| *α*, *β*, *γ* (°) | 90.0, 90.0, 90.0 | 90.0, 90.0, 90.0 | 90.0, 90.0, 90.0 | 90.0, 90.0, 90.0 |
| Wavelength (Å) | 0.9794 | 0.9794 | 0.9794 | 0.9794 |
| Resolution (Å) | 50–2.66 (2.71–2.66)[a] | 50–1.92 (1.95–1.92)[a] | 50–1.95 (1.98–1.95)[a] | 50–2.22 (2.26–2.22)[a] |
| Unique reflections | 34,177 | 88,457 | 78,678 | 54,859 |
| $R_{sym}$ or $R_{merge}$ | 0.079 (0.677) | 0.054 (0.638) | 0.039(0.435) | 0.113 (0.893) |
| $I/\sigma I$ | 27.2 (2.0) | 28.3 (2.0) | 41.0 (2.4) | 19.0 (2.2) |
| Completeness (%) | 99.5 (96.0) | 99.3 (91.6) | 92.2(61.4) | 98.6 (93.3) |
| Redundancy | 6.2 (4.4) | 6.1 (4.9) | 5.8 (3.9) | 6.4 (4.3) |
| **Refinement** | | | | |
| Resolution (Å) | 47.71–2.66 | 45.86–1.92 | 45.94–1.95 | 46.36–2.22 |
| No. reflections | 31,782/2,845 | 80,503/3,225 | 72,649/3,030 | 47,829/3,179 |
| $R_{work}/R_{free}$ | 0.2246/0.2784 | 0.1801/0.2228 | 0.1621/0.2046 | 0.1781/0.2170 |
| No. atoms | 6,816 | 7,976 | 7,894 | 7,497 |
| Protein | 6,584 | 7,241 | 7,219 | 7,155 |
| Ligand/ion | 56 | 56 | 56 | 60 |
| Water | 176 | 679 | 619 | 282 |
| *B*-factors | 35.33 | 34.40 | 32.33 | 46.40 |
| Protein | 35.35 | 34.15 | 32.15 | 46.66 |
| Ligand/ion | 41.62 | 25.29 | 18.54 | 38.19 |
| Water | 32.26 | 37.85 | 35.73 | 41.76 |
| R.m.s. deviations | | | | |
| Bond lengths (Å) | 0.003 | 0.004 | 0.004 | 0.003 |
| Bond angles (°) | 0.715 | 0.664 | 0.672 | 0.577 |

[a] Values in parentheses are for highest-resolution shell.

membrane and for maintaining the proton-motive force [14]. Because conservation of prokaryotic gene clusters between genomes is a strong indicator of functional association [15], it is tempting to speculate that the YcjXF pair may work together with the Psp system in maintaining inner membrane function during envelope stress [16].

## YcjX is a GTP hydrolase

Despite being a major stress protein, the three-dimensional structure of YcjX has remained elusive. A structure-prediction search of the Protein Data Bank using HHpred [17] did not reveal a homologous protein of known structure, prompting us to pursue the crystal structure determination of YcjX. Owing to our interest in *S. oneidensis*, we amplified the open reading frame of *S. oneidensis ycjX* from genomic DNA and cloned the gene into a customized vector to facilitate the soluble overexpression of YcjX in *E. coli*. YcjX was purified using a three-step column chromatography procedure followed by size-exclusion chromatography (Fig. 1b). The SEC-MALS analysis showed that YcjX elutes as a 58.3-kDa protein, which is similar to its calculated molecular weight of 54.6 kDa, indicating that YcjX is a monomer in solution. In addition, because P-loop containing proteins typically bind ATP or GTP, we determined the ability of YcjX to hydrolyze nucleotides in the absence or presence of 5 mM $MgCl_2$. We found that only in the presence of magnesium ions does YcjX slowly hydrolyze GTP, but not ATP (Fig. 1c), demonstrating that YcjX is not an ATPase.

## Crystal structure of *S. oneidensis* YcjX

*S. oneidensis* YcjX was crystallized at 14 °C by the hanging-drop vapor diffusion method. We obtained crystals under a wide variety of different chemical conditions irrespective of what guanine nucleotide, if any, was added. We used 20 crystals for structure analysis, each one obtained under different crystallization conditions. Although crystals were non-isomorphous, they all belonged to the same space group, $P2_12_12_1$, with two molecules of YcjX in the crystallographic asymmetric unit (Table 1). For each crystal, mol-A superposes onto mol-B with an RMSD of only 0.55 ± 0.07 Å over 417 Cα atoms, indicating that the two molecules are largely identical. The experimental map enabled tracing of all residues except for the 18 N-terminal amino acids in mol-A and the first 23 amino acids in mol-B, as well as a loop region consisting of residues 57–65 that was disordered in both YcjX copies.

Each YcjX molecule shares at its core the monomeric GTPase domain of Ras, featuring the canonical P-loop (residues 33–40), switch 1 (residues 110–120), and switch 2 (residues 148–

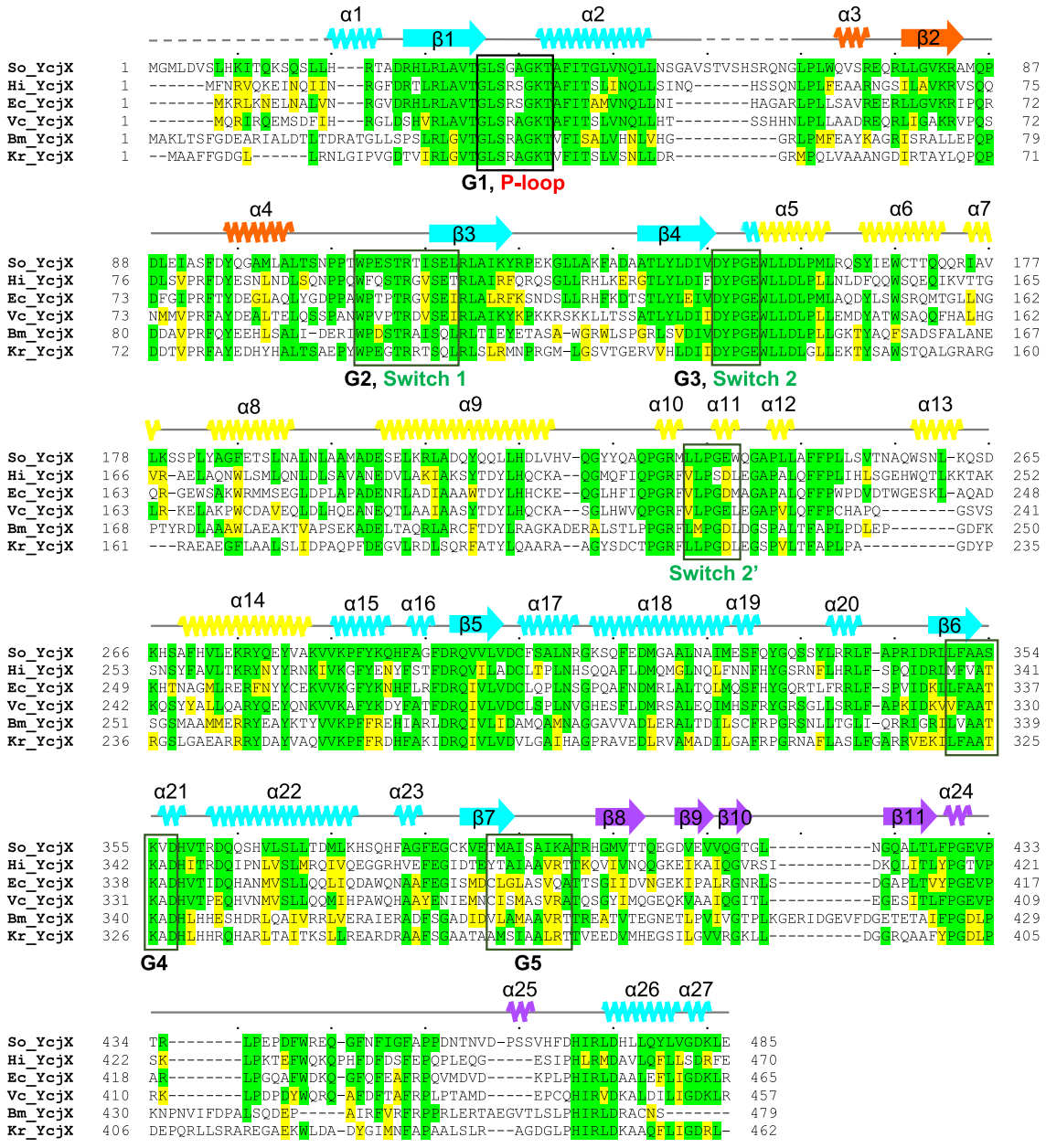


**Fig. 2.** YcjX is a conserved stress-induced protein in gram-negative bacteria. Multiple-sequence alignment of YcjX from *S. oneidensis* (So), *Haemophilus influenzae* (Hi), *E. coli* (Ec), *Vibrio cholerae* (Vc), *Brucella melitensis* (Bm), and *Ketogulonicigenium robustum* (Kr). Conserved and similar residues are highlighted in green and yellow, respectively. The dot marks every 10th amino acid. Secondary structure elements are shown as helices (α-helix) and arrows (β-strand), and are colored according to domain assignment: GTPase domain in cyan, N-terminal insertion in orange, α-helical insertion in yellow, and C-terminal insertion in purple. The same colors are used throughout in all figures.

152) motifs required for GTP binding and hydrolysis (Fig. 2). The core domain consists of a six-stranded β-sheet with five strands running parallel and one (β3) running antiparallel to the others and is flanked by α-helices on either surface (Fig. 3a and b). Interestingly, the YcjX core domain features both an N-terminal alpha-beta-alpha insertion (residues 53–109) preceding switch 1 and a C-terminal alpha-beta domain insertion (residues 401–470) that deviates from the canonical Ras fold (Fig. 3b). In the crystal structure, the C-terminal insertion wraps around the core domain, placing the N- and C-termini in close proximity, ~15 Å apart (Fig. 3a).

Most strikingly, instead of the conserved helix 2 of Ras (Fig. 3c), YcjX features a ~131-amino-acid, α-helical domain comprising residues 153–283 (Fig.

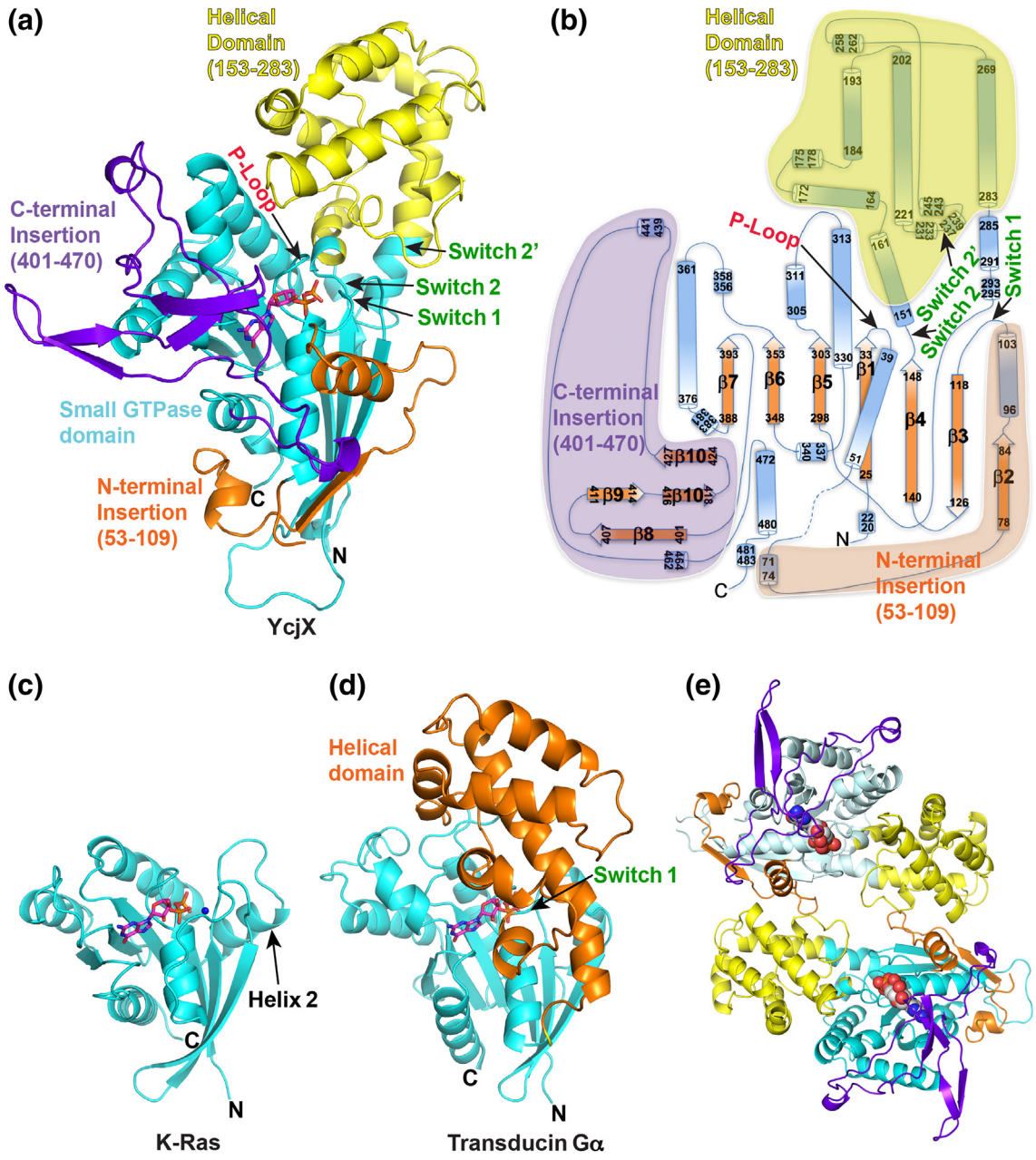


**Fig. 3.** Crystal structure of YcjX. (a) Ribbon diagram of YcjX with secondary structure elements colored according to domain assignment. Locations of the P-loop, switch 1, switch 2, and switch 2′ are shown. GDP is depicted as stick model. (b) Topology diagram of YcjX. Secondary structure elements are shown as blue helices (α-helix) and orange arrows (β-strand). The N-terminal (orange), helical (yellow), and C-terminal insertions (purple) not found in other G proteins are shaded. (c) Ribbon diagram of human K-Ras bound to GDP (PDB ID: 5W22) [31]. (d) Ribbon diagram of the Gα subunit of bovine Transducin bound to GDP (PDB ID: 1TAG) [18]. (e) Ribbon diagram of the two copies of YcjX in the crystallographic asymmetric unit. GDP is shown as CPK model.

3a and b). The helical domain insertion immediately follows switch 2 and features a mobile loop flanked by short α-helices, which we term switch 2′ (residues 234–239). We note that the helical domain insertion in YcjX resembles the helical domain of the α-subunit (Gα) of Transducin [18] (Fig. 3d) but is found in a different location in the three-dimensional structure (Fig. S1). In Gα, the helical domain precedes switch 1 and clamps the nucleotide in a deep cleft, which was proposed to account for the negligible thermal exchange rate of bound nucleotide [6]. To our knowledge, YcjX is the first example

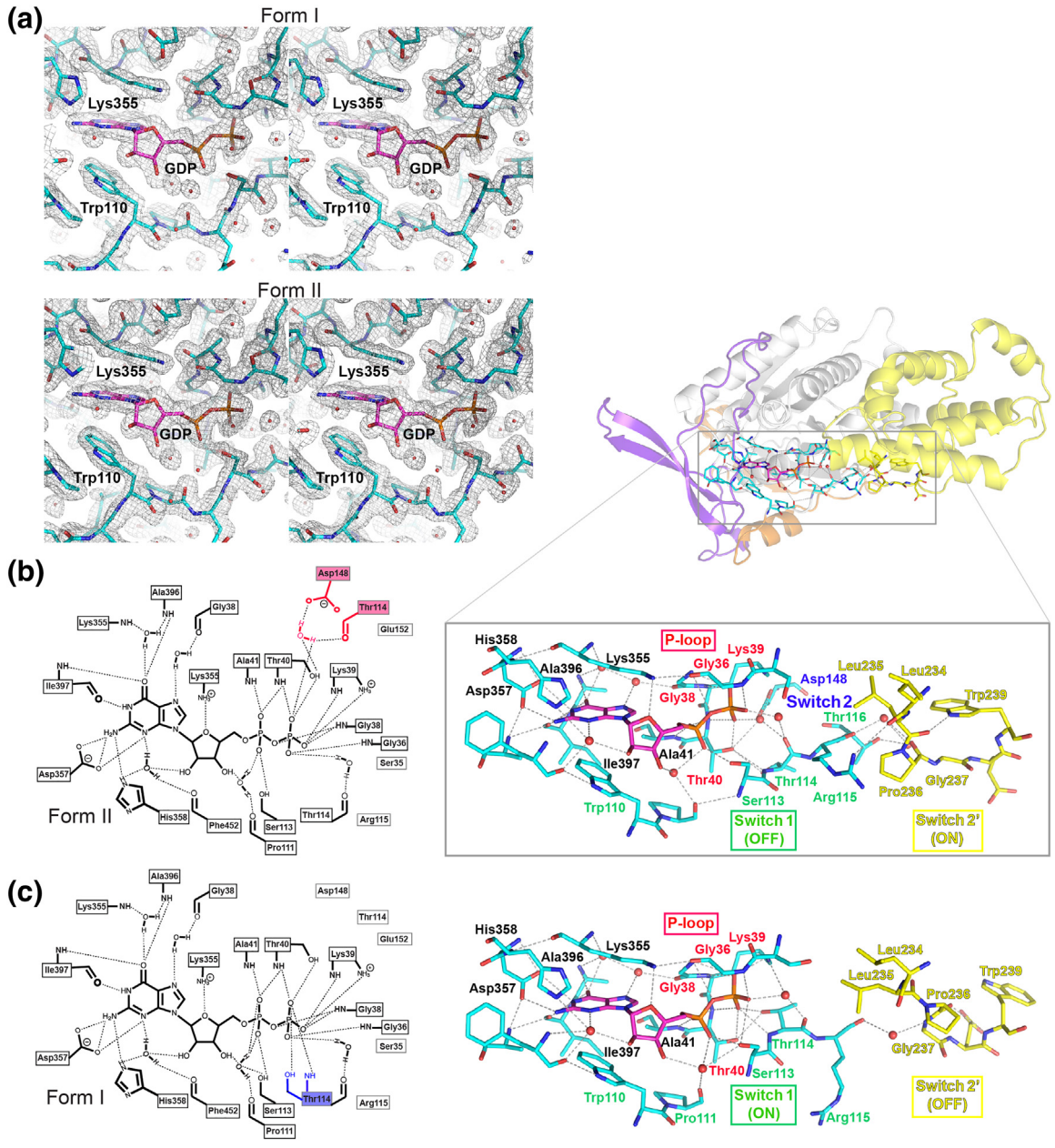


**Fig. 4.** YcjX•GDP adopts two different conformations. (a) Stereo drawings of the nucleotide binding cleft in GDP-Form I and GDP-Form II. The simulated annealing composite omit maps are shown as gray mesh and are contoured at 1.5 $\sigma$. (b) Ribbon diagram of YcjX GDP-Form II with close-up view of the nucleotide-binding site. Switch 1 and switch 2′ are in the "OFF/ON" position. The schematic diagram depicts all polar interactions between YcjX and bound GDP. (c) Close-up view of the nucleotide-binding site of YcjX GDP-Form I. Switch 1 and switch 2′ are in the "ON/OFF" position. Polar interactions that differ between GDP-Form I and GDP-Form II are colored in the schematic diagram.

of a bacterial G protein featuring a helical domain insertion outside the Gα subunit (Fig. S2). In the crystal structure of YcjX, the helical domain stacks against the core domain of its symmetry neighbor (Fig. 3e). Because YcjX is a monomer in solution (Fig. 1b), the observed interaction is non-physiological but could be indicative of binding to an unknown effector protein.

## The GDP-bound conformation

YcjX crystallized with two copies in the asymmetric unit. Surprisingly, both YcjX monomers are bound to GDP even when no nucleotide was added for crystallization, suggesting that GDP co-purified from the expression host. Addition of GDP or GDP•AlFx during crystallization yielded similar

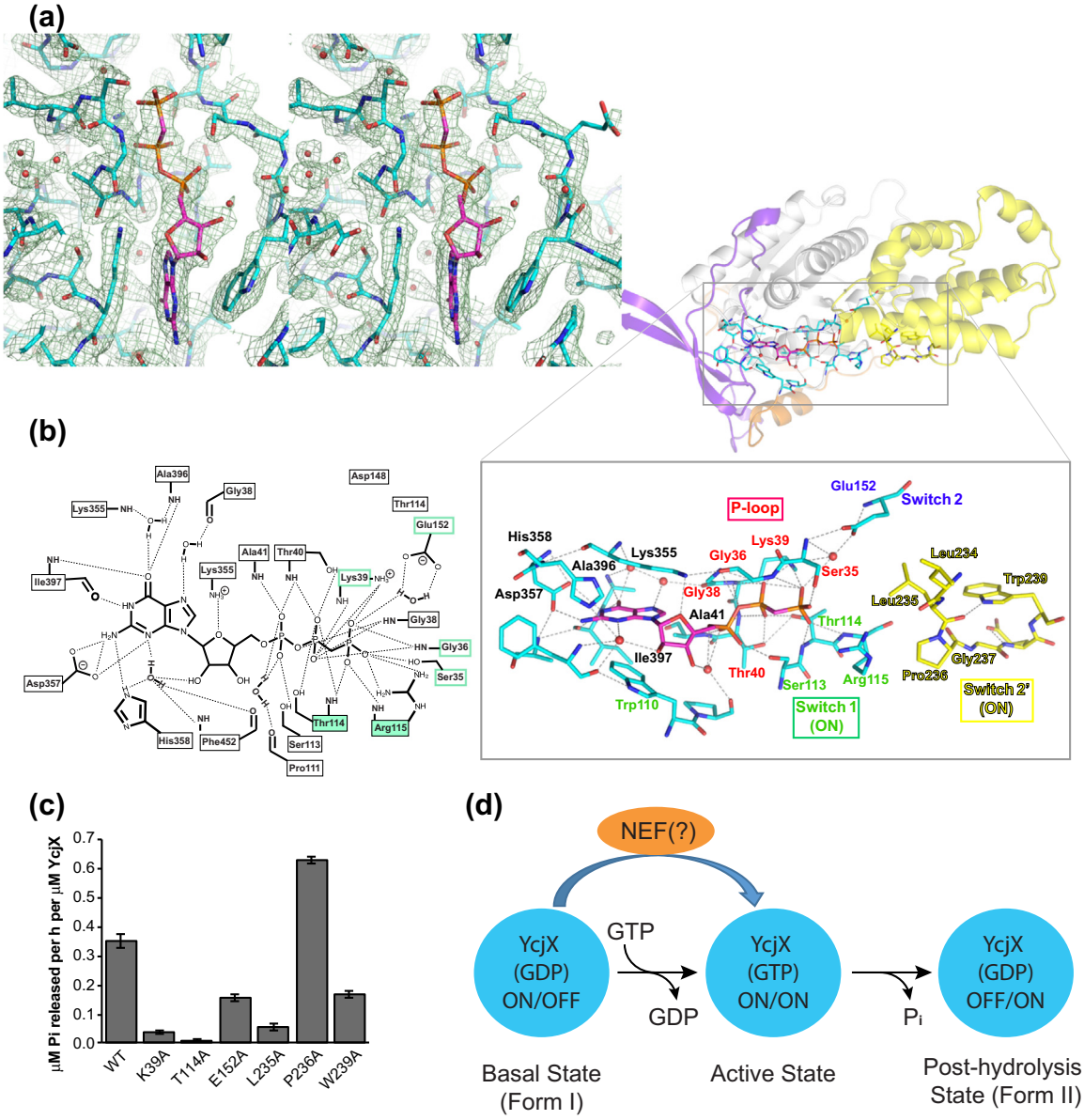


**Fig. 5.** The crystal structure of the GDPCP-bound state shows YcjX in an active conformation. (a) Stereo drawing of the nucleotide binding cleft. The simulated annealing composite omit map is shown as green mesh and is contoured at 1.5 σ. (b) Ribbon diagram of YcjX•GDPCP. The inset shows an enlarged segment of the nucleotide binding site with switch 1 and switch 2′ in the "ON/ON" conformation. The schematic diagram depicts all polar interactions between YcjX and bound GDPCP. Polar interactions contacting the γ-phosphate are colored. (c) GTPase activities of YcjX wild type and mutant proteins. Averages of three independent measurements (n = 3) ± SD are shown. (d) Proposed model for the switching mechanism underlying YcjX activation. The model assumes that YcjX•GDPCP represents the fully active conformation with both switch 1 and switch 2′ in the "ON/ON" state. The model predicts that an exchange of GDP for GTP, catalyzed by a nucleotide exchange factor (NEF), activates switch 2′. GTP hydrolysis concomitant with Pi release causes switch 1 to change into the inactive state.

crystals, with crystals diffracting to 1.95-Å resolution or better (Table 1). However, in all cases, only bound GDP was observed in the electron density with the guanosine moiety sandwiched between the side chains of Trp110 and Lys355 (Fig. 4a). The peptide NH groups of Ala396 and Ile397 confer base specificity by donating hydrogen bonds to the 6-oxo substituent of the guanine base, with the Asp357 side chain and Ile397 main chain carbonyl accepting a hydrogen bond from the 2-amino group and the N1 amine, respectively. In addition, the side chain of His358 in its protonated form can donate a hydrogen

bond to the 2-amino group of the bound guanine nucleotide (Fig. 4b and c). The phosphate moiety of GDP is clamped between switch 1 and P-loop residues 36–41 with the side chain OH of Ser113 and the main chain NH of both Thr40 and Ala41 donating hydrogen bonds to the α-phosphate. In addition, the main chain NH of Gly36, Gly38, Lys39, and Thr40 along with the side chains of Lys39 and Thr40 donate hydrogen bonds to the β-phosphate of GDP (Fig. 4b and c). Surprisingly, we did not observe a bound magnesium ion coordinating the α- and β-phosphates of GDP in any of the 20 refined crystal structures of YcjX determined during the course of this work (Fig. S3). However, lack of $Mg^{2+}$ binding is not unprecedented and a bound $Mg^{2+}$ is also not observed in crystal structures for the Ras-related ARL3 [19] and MglA GTPases [20]. Although a majority of G protein structures contain a bound magnesium ion [7], it appears that $Mg^{2+}$ is dispensable for nucleotide binding by YcjX.

## Structures of YcjX•GDP in two different switch conformations

Surprisingly, we found that YcjX crystallized in two different GDP-bound conformations (GDP-Form I and GDP-Form II). Although each Form I monomer superposed pairwise onto a Form II monomer with an RMSD of only 0.59 ± 0.12 Å over 415 Cα atoms, the GDP-Form I and GDP-Form II conformers differed in their respective switch 1 and switch 2′ conformations (compare Fig. 4b with c). No structural differences in the canonical switch 2 region were observed. Switch 2′ is located within the novel helical domain insertion and is adjacent to switch 2 in the three-dimensional structure. In GDP-Form II, the side chain of the conserved Thr114 (switch 1) faces away from the α/β-phosphate, resembling the switch 1 conformation of the GDP-bound state in the crystal structure of the Gα subunit of Transducin [18]. While switch 1 is in the so-called "OFF" state, the Arg115 side chain donates a hydrogen bond to the main chain carbonyl of Leu234 and is in van der Waals contact with Pro236, pulling switch 2′ toward the bound nucleotide as might be expected for an activated "ON" state. The conformation of switch 2′ is further stabilized by two water-mediated interactions of the peptide carbonyl of Pro236 with the main chain carbonyl of Arg115 and the side chain of Thr116 (Fig. 4b).

In GDP-Form I, the switch 1 region is pulled toward the bound nucleotide with both the peptide NH and side chain OH of the conserved Thr114 donating hydrogen bonds to the β-phosphate. Notably, this switch 1 conformation is similar to the activated "ON" state of the Gα subunit with triphosphate [6] and contrasts the aforementioned switch 1 conformation in GDP-Form II. Concomitant with an alternate switch 1 conformation, Pro236 is flipped, resulting in a conformational change of switch 2′ (Fig. 4c). Now, the peptide NH of Gly237 makes a water-mediated contact with the main chain carbonyl of Arg115, whose side chain is moved away from the bound nucleotide, reminiscent of the inactive "OFF" state.

Taken together, we observed two different YcjX•GDP conformations, representing structures of the ON/OFF (GDP-Form I; Fig. 4c) and OFF/ON state (GDP-Form II; Fig. 4b). Other segments of the YcjX•GDP structure, including the P-loop and switch 2 region, remain unchanged.

## The GTP-bound conformation

It is entirely fortuitous, although not surprising, that YcjX crystallized with bound GDP. It was previously reported that bacterially expressed, recombinant Ras co-purified with GDP, which thereby may have stabilized the protein [21]. Owing to the high affinity of YcjX for guanine nucleotide, our attempts to crystallize YcjX with other nucleotides by nucleotide addition were unsuccessful.

To determine the crystal structure of YcjX in the GTP conformation, we pretreated YcjX with alkaline phosphatase in the presence of GDPCP. It was previously shown that this procedure removes tightly bound guanine nucleotides from GTP-binding proteins and replaces it with GTP analogs resistant to alkaline phosphatase treatment [21,22]. Following this procedure, we obtained crystals of YcjX•GDPCP and determined its structure at 2.2-Å resolution by molecular replacement (Fig. 5a). Although YcjX•GDPCP crystallized under chemically distinct conditions, the crystals belonged to the same orthorhombic space group with similar unit cell dimensions, containing two molecules in the asymmetric unit. The simulated annealing composite omit map clearly shows the γ-phosphate group of GDPCP bound to mol-A (Fig. 5a). However, the γ-phosphate group of the bound nucleotide is only partially visible in mol-B and was therefore modeled as GDP. We speculate that this heterogeneous occupancy may have resulted from an incomplete nucleotide exchange procedure. Similar to the crystal structure of the GDP-bound states, we did not observe bound $Mg^{2+}$ in either mol-A or mol-B, indicating that magnesium is dispensable for nucleotide binding, consistent with previous reports for selected monomeric GTPases [19,20].

Pairwise comparison of mol-A and mol-B shows that the two structures are nearly identical (RMSD of only 0.60 Å) but differ in their switch 2′ conformations. Mol-B is highly similar to the structure of GDP-Form I with switch 1 and switch 2′ in the ON/OFF state. However, in mol-A, switch 1 and switch 2′ are in the ON/ON conformation as would be expected for the activated GTP-bound state, with the main chain NH of both Thr114 and Arg115 and the side chains

of Lys39 and Arg115 donating hydrogen bonds to the γ-phosphate (Fig. 5b). Glu152 (switch 2) makes an important water-mediated contact with the γ-phosphate of the bound GDPCP. No other changes in the P-loop or switch 2 conformation are observed. To determine whether the non-canonical switch 2′ motif is essential for catalysis, we created YcjX with mutations at Leu235, Pro236, or Trp239 to alanine and examined the ability of these single-point mutants to hydrolyze GTP. We found that the L235A and W239A mutants abolished or significantly impaired the GTPase activity similar to levels observed with the P-loop (K39A) and switch 2 (E152A) mutants, respectively (Fig. 5c). As anticipated, mutating the invariant Thr114 (switch 1) completely abolished GTP hydrolysis. In contrast, the P236A mutant stimulated the YcjX's GTPase activity 1.8-fold (Fig. 5c). Although the nature of this stimulation remains unclear, our findings demonstrate that all three nucleotide switch motifs of YcjX are mutationally sensitive, consistent with a key role in GTP binding, hydrolysis, or both.

## Discussion

The crystal structure of YcjX provides the first atomic snapshot of a member of the DUF463 family of stress-activated proteins ubiquitously found in gram-negative proteobacteria (Fig. 2). We show that YcjX is not an ATPase, but a GTP-binding protein. Because molecular chaperones typically harness ATP as energy source, our findings argue against the notion that YcjX plays a direct role in protein folding. YcjX shares the GTP-binding domain of Ras at its core but features several novel insertions, including an α-helical domain not found in other monomeric GTPases. In this regard, the structure of YcjX is reminiscent of the Gα subunit in heterotrimeric G proteins [6,23], although the topology and location of the helical domain insertions are different.

Structural analysis of G proteins in their di- and triphosphate states has previously showed that guanine nucleotide-dependent changes in protein conformation are confined to the evolutionary conserved switch 1 and switch 2 motifs [7,23]. While the YcjX switch 1 conformation in the GDP-"OFF" and GDPCP-"ON" states resembles the switch 1 conformation in the crystal structures of Transducin Gα with di- or triphosphate [6], no conformational changes in switch 2 are observed. Observed differences are confined to the conserved switch 1 motif and the novel switch 2′ motif that is located within the α-helical domain outside of the canonical Ras fold. Our targeted mutagenesis confirmed the catalytic importance of the switch 1 and switch 2′ motifs (Fig. 5c). This finding was unexpected and suggests that YcjX utilizes a non-canonical nucleotide switch mechanism, distinct from the evolutionary conserved model [7,24].

We propose that the three distinct YcjX conformations in the ON/OFF (GDP-Form I), ON/ON (GDPCP), and OFF/ON state (GDP-Form II) represent snapshots of different functional states during the GTP hydrolysis cycle (Fig. 5d). In our model, the structure of the inactive OFF/OFF state would be represented by nucleotide-free YcjX, which is never observed due to the high affinity of YcjX for GDP present in cells or from GTP that is readily hydrolyzed [7]. Hence, the basal state with GDP essentially represents the structure of inactive YcjX under physiological conditions. YcjX activation requires binding of guanine triphosphate and is likely catalyzed by a guanine nucleotide-exchange factor, whose identity remains unknown (Fig. 5d). Following GTP hydrolysis, switch 1 returns to its inactive state depicted by GDP-Form II, which may represent a post-hydrolysis conformation.

Although our model is consistent with the known role of guanine nucleotides in G protein activation, we cannot rule out the possibility of spontaneous switching between GDP-Form I and GDP-Form II, which may exist in equilibrium. Nevertheless, it is already apparent that YcjX differs from Ras-like GTPases by utilizing a non-canonical switch 2′ motif not found in other G proteins. In light of the close gene association between *ycjX* and *ycjF* (Fig. 1a), it is tempting to speculate that YcjX may function as a transducer of transmembrane receptor-generated stress response signals, akin to the role of Gα in G-protein-coupled receptor signaling, which is subject to further investigation.

## Materials and Methods

### Cloning

The ORF of *ycjX* (SO1810) was PCR amplified from *S. oneidensis* strain MR-1 genomic DNA (American Type Culture Collection). *YcjX* was cloned into a modified pPROEX Htb vector harboring a TEV protease cleavable, N-terminal $His_6$-SUMO tag. DNA sequencing revealed two unintended mutations, F187L and D218G, which were corrected by QuikChange site-directed mutagenesis to make the wild-type protein. All YcjX mutants were generated from the wild-type gene using QuikChange.

### Protein expression and purification

p$His_6$-SUMO-YcjX was freshly transformed into *E. coli* BL21-CodonPlus(DE3)-RIL cells. Cultures were grown from a single colony at 37 °C in LB medium to an $OD_{600}$ of 0.5–0.6 and cooled down to 16 °C. YcjX expression was induced with 0.3 mM IPTG, and cells

continued growing for an additional 14 h before harvesting. The cell pellet was resuspended in lysis buffer [25 mM Tris (pH 8.0), 300 mM NaCl, 30 mM imidazole, 5 mM β-mercaptoethanol] and lysed using a microfluidizer processor. The cleared lysate was applied to a pre-equilibrated Ni-sepharose HP column (25 ml) and washed with 30 column volumes of lysis buffer. YcjX was eluted over a linear gradient of 30–300 mM imidazole. After elution, the N-terminal $His_6$-SUMO tag was cleaved off overnight and dialyzed against 25 mM Tris (pH 8.5), 200 mM NaCl, and 5 mM β-mercaptoethanol. The dialyzed sample was reapplied onto a Ni-sepharose HP column to remove the liberated His-tag, His-TEV protease and any uncleaved protein. YcjX was further purified on a Mono-Q column (GE Healthcare) and eluted over a linear gradient of 0–1.0 M NaCl in 25 mM Tris (pH 8.8) and 5 mM β-mercaptoethanol. The peak fraction eluted around 180 mM NaCl and was concentrated prior to crystallization to 8 mg/ml calculated using a molar extinction coefficient of 60,850 $M^{-1}$ $cm^{-1}$ ($A_{280}$). The same expression and purification procedure was used for all YcjX mutants. Se-Met substituted YcjX was prepared by transforming an *E. coli* methionine auxotroph strain, B834-CodonPlus(DE3)-RIL pLysS. Cells were grown in defined medium supplemented with 50 mg/L seleno-DL-methionine. Preparation of Se-Met YcjX was otherwise identical to native YcjX.

### Size exclusion chromatography

The oligomerization state of YcjX (320 μM) was determined by analytical SEC using a Superdex 200 10/300 column (GE Healthcare) pre-equilibrated in 25 mM Tris (pH 8.8), 100 mM NaCl, and 5 mM β-mercaptoethanol. The SEC-MALS analysis was performed at the Core for Biomolecular Structure and Function at the University of Texas MD Anderson Cancer Center.

### GTPase activity assay

YcjX wild-type and mutants (20 μM) in 50 mM Tris (pH 8.8), 180 mM NaCl, and 5 mM β-mercaptoethanol were incubated with either 1 mM GTP or 2 mM ATP at 22 °C for 6 h in the absence or presence of 5 mM $MgCl_2$. The amount of released inorganic phosphate was measured using the malachite green assay.

### Alkaline phosphatase treatment

To make the YcjX•GDPCP complex, YcjX•GDP (2 mg, 8 mg/ml) in 25 mM Tris (pH 8.8), 200 mM NaCl, and 5 mM β-mercaptoethanol was incubated with 4 units of alkaline phosphatase-agarose (Sigma-Aldrich) and 1 mM GDPCP at 25 °C. Degradation of GDP was monitored by the malachite green assay until no inorganic phosphate was released. Alkaline phosphatase-agarose was removed by centrifugation, and an additional 4 mM GDPCP was added to the sample prior to crystallization.

### Crystallization and data collection

Crystals of YcjX were grown at 14 °C by the hanging drop vapor diffusion method by mixing 1 μl of protein solution (8 mg/ml) in 25 mM Tris (pH 8.8), 180 mM NaCl, 10 mM $MgCl_2$, and 5 mM β-mercaptoethanol with or without 5 mM guanine nucleotide (GDP, GDPNP, or GDPCP) and an equal volume of precipitant solution over a 100-μl reservoir. Data from crystals presented here were obtained in 50 mM sodium succinate (pH 5.0), 500 mM NaCl, and 20% (v/v) PEG 400 (Se-Met); 50 mM MES (pH 6.0), 400 mM ammonium chloride, and 15% (w/v) MePEG 2000 (GDP-Form I); 50 mM sodium cacodylate (pH 6.5), 50 mM MES (pH 6.0), and 27.5% (v/v) PEP426 (GDP-Form II); and 100 mM HEPES (pH 6.5) and 6% (w/v) polyvinyl pyrrolidone (GDPCP). All crystals obtained belonged to the primitive orthorhombic space group, $P2_12_12_1$ with similar unit cell parameters. For data collection, crystals were harvested in reservoir solution (GDP-Form II), or reservoir solution supplemented with 35% (v/v) PEG400 (Se-Met), 20% (v/v) glycerol (GDP-Form I), or 25% (v/v) glycerol (GDPCP) and flash frozen in liquid nitrogen. A 2.66-Å resolution SAD data set near the selenium absorption peak (0.9794 Å) and native data sets at 1.92-Å (GDP-Form I), 1.95-Å (GDP-Form II), and 2.22-Å resolution (GDPCP) were collected at 100 K at the APS SBC ID19 beamline equipped with a Dectris Pilatus 6M detector. All data were processed using HKL3000 [25].

### Structure solution and refinement

SAD phasing, density modification (DM), and initial model building were done using the structure module of the HKL3000 software package [25]. A total of 21 selenium sites were located using SHELXD [26]. Initial phases were calculated using MLPHARE [27], yielding a mean figure of merit of 0.211 for data between 50- and 3.07-Å resolution, which was further improved to 0.781 for data between 50- and 2.66-Å resolution after DM. The script build module in Buccaneer [28] was used to build 1008 residues and place the side chains of 829 residues. The initial model was rebuilt in COOT [29] using electron density maps calculated with the DM-phased reflection file. After each cycle of rebuilding, the model was refined using PHENIX [30]. Native structures (GDP-Form I, GDPCP, and GDP-Form II) were determined subsequently by molecular replacement using the partially refined structure of Se-Met YcjX as a search model. The refined structures have excellent stereochemical properties

with 97.26% and 2.74% (GDP-Form I), 97.01% and 2.99% (GDPCP), and 98.00% and 2.00% (GDP-Form II) of residues either in most favored or allowed regions, and none of the residues in disallowed regions of the Ramachandran plot.

### Accession numbers

Atomic coordinates and accompanying structure factors for YcjX in the GDP-Forms I, GDPCP, and GDP-Form II conformations have been deposited with the RCSB with access codes PDB ID: 6NZ4, PDB ID: 6NZ5, and PDB ID: 6NZ6.

## CRediT authorship contribution statement

**Joshua T. Tsai:** Conceptualization, Investigation, Formal analysis, Writing - original draft, Writing - review & editing. **Nuri Sung:** Investigation. **Jungsoon Lee:** Investigation, Formal analysis, Writing - original draft. **Changsoo Chang:** Investigation. **Sukyeong Lee:** Investigation, Formal analysis, Funding acquisition, Supervision, Writing - original draft, Writing - review & editing. **Francis T.F. Tsai:** Funding acquisition, Supervision, Writing - original draft, Writing - review & editing.

## Acknowledgments

We thank Dr. P. Leonard for performing the SEC-MALS analysis. This work was supported by the Macromolecular Crystallography Core at Baylor College of Medicine and by grants from the National Institutes of Health (R01-GM111084 and P01-HD087157) and the Welch Foundation (Q-1530). Use of the SBC beamlines at the Advanced Photon Source was supported by the U.S. Department of Energy Office of Science under Contract No. DE-AC02-06CH11357.

**Declarations of Interest:** None.

## Appendix A. Supplementary data

Supplementary data to this article can be found online at https://doi.org/10.1016/j.jmb.2019.06.006.

*Received 17 February 2019;*
*Received in revised form 11 May 2019;*
*Available online 14 June 2019*

***Keywords:***
G-proteinRas;
GTPasestress signaling

***Abbreviations used:***
Se-Met, seleno-methionine; Psp, phage-shock-protein; DM, density modification.

## References

[1] D. Balchin, M. Hayer-Hartl, F.U. Hartl, In vivo aspects of protein folding and quality control, Science 353 (2016) aac4354.
[2] G. Nonaka, M. Blankschien, C. Herman, C.A. Gross, V.A. Rhodius, Regulon and promoter analysis of the *E. coli* heat-shock factor, sigma32, reveals a multifaceted cellular response to heat stress, Genes Dev. 20 (2006) 1776–1789.
[3] A. Rasouly, M. Schonbrun, Y. Shenhar, E.Z. Ron, YbeY, a heat shock protein involved in translation in *Escherichia coli*, J. Bacteriol. 191 (2009) 2649–2655.
[4] A. Rasouly, E.Z. Ron, Interplay between the heat shock response and translation in *Escherichia coli*, Res. Microbiol. 160 (2009) 288–296.
[5] U. Choi, Y.H. Park, Y.R. Kim, Y.J. Seok, C.R. Lee, Increased expression of genes involved in uptake and degradation of murein tripeptide under nitrogen starvation in *Escherichia coli*, FEMS Microbiol. Lett. 363 (2016) fnw136.
[6] P.B. Sigler, Stereochemistry of activation and GTPase mechanisms of Gtα at 1.8 Å resolution, in: T.W. Schwartz, S.A. Hjorth, J. Sandholm Kastrup (Eds.), Alfred Benzon Symposium, Munksgaard, Copenhagen 1996, pp. 17–29.
[7] A. Wittinghofer, I.R. Vetter, Structure-function relationships of the G domain, a canonical switch motif, Annu. Rev. Biochem. 80 (2011) 943–971.
[8] W. Jeng, S. Lee, N. Sung, J. Lee, F.T.F. Tsai, Molecular chaperones: guardians of the proteome in normal and disease states, F1000Res. 4 (2015) 1448.
[9] K. Liu, A.N. Bittner, J.D. Wang, Diversity in (p)ppGpp metabolism and effectors, Curr. Opin. Microbiol. 24 (2015) 72–79.
[10] A.L. Mitchell, T.K. Attwood, P.C. Babbitt, M. Blum, P. Bork, A. Bridge, et al., InterPro in 2019: improving coverage, classification and access to protein sequence annotations, Nucleic Acids Res. 47 (2019) D351–D360.
[11] J.E. Walker, M. Saraste, M.J. Runswick, N.J. Gay, Distantly related sequences in the alpha- and beta-subunits of ATP synthase, myosin, kinases and other ATP-requiring enzymes and a common nucleotide binding fold, EMBO J. 1 (1982) 945–951.
[12] M.A. Khan, R.E. Isaacson, Identification of *Escherichia coli* genes that are specifically expressed in a murine model of septicemic infection, Infect. Immun. 70 (2002) 3404–3412.
[13] A.J. Darwin, The phage-shock-protein response, Mol. Microbiol. 57 (2005) 621–628.
[14] M. Huvet, T. Toni, X. Sheng, T. Thorne, G. Jovanovic, C. Engl, et al., The evolution of the phage shock protein response system: interplay between protein function, genomic organization, and system function, Mol. Biol. Evol. 28 (2011) 1141–1155.
[15] R. Overbeek, M. Fonstein, M. D'Souza, G.D. Pusch, N. Maltsev, The use of gene clusters to infer functional coupling, Proc. Natl. Acad. Sci. U. S. A. 96 (1999) 2896–2901.
[16] R. Manganelli, M.L. Gennaro, Protecting from envelope stress: variations on the phage-shock-protein theme, Trends Microbiol. 25 (2017) 205–216.
[17] L. Zimmermann, A. Stephens, S.Z. Nam, D. Rau, J. Kübler, M. Lozajic, et al., A completely reimplemented MPI

bioinformatics toolkit with a new HHpred server at its core, J. Mol. Biol. 430 (2018) 2237–2243.
[18] D.G. Lambright, J.P. Noel, H.E. Hamm, P.B. Sigler, Structural determinants for activation of the alpha-subunit of a heterotrimeric G protein, Nature 369 (1994) 621–628.
[19] R.C. Hillig, M. Hanzal-Bayer, M. Linari, J. Becker, A. Wittinghofer, L. Renault, Structural and biochemical properties show ARL3-GDP as a distinct GTP binding protein, Structure 8 (2000) 1239–1245.
[20] M. Miertzschke, C. Koerner, I.R. Vetter, D. Keilberg, E. Hot, S. Leonardy, et al., Structural analysis of the Ras-like G protein MglA and its cognate GAP MglB and implications for bacterial polarity, EMBO J. 30 (2011) 4185–4197.
[21] J. John, R. Sohmen, J. Feuerstein, R. Linke, A. Wittinghofer, R. S. Goody, Kinetics of interaction of nucleotides with nucleotide-free H-ras p21, Biochemistry 29 (1990) 6058–6065.
[22] D.L. Purich, R.K. MacNeal, Properties of tubulin treated with alkaline phosphatase to remove guanine nucleotides from the exchangeable binding site, FEBS Lett. 96 (1978) 83–86.
[23] S.R. Sprang, Invited review: Activation of G proteins by GTP and the mechanism of Gα-catalyzed GTP hydrolysis, Biopolymers 105 (2016) 449–462.
[24] W.M. Oldham, H.E. Hamm, Heterotrimeric G protein activation by G-protein-coupled receptors, Nat. Rev. Mol. Cell Biol. 9 (2008) 60–71.
[25] W. Minor, M. Cymborowski, Z. Otwinowski, M. Chruszcz, HKL-3000: the integration of data reduction and structure solution - from diffraction images to an initial model in minutes, Acta Crystallogr. D Biol. Crystallogr. 62 (2006) 859–866.
[26] G.M. Sheldrick, Experimental phasing with SHELXC/D/E: combining chain tracing with density modification, Acta Crystallogr. D Biol. Crystallogr. 66 (2010) 479–485.
[27] Z. Otwinowski, Maximum likelihood refinement of heavy atom parameters, in: W. Wolf, P.R. Evans, A.G.W. Leslie (Eds.), Isomorphous Replacement and Anomalous Scattering, Daresbury Laboratory, Warrington 1991, pp. 80–86.
[28] K. Cowtan, The Buccaneer software for automated model building. 1. Tracing protein chains, Acta Crystallogr. D Biol. Crystallogr. 62 (2006) 1002–1011.
[29] P. Emsley, K. Cowtan, Coot: model-building tools for molecular graphics, Acta Crystallogr. D Biol. Crystallogr. 60 (2004) 2126–2132.
[30] P.D. Adams, P.V. Afonine, G. Bunkóczi, V.B. Chen, I.W. Davis, N. Echols, et al., PHENIX: a comprehensive Python-based system for macromolecular structure solution, Acta Crystallogr. D Biol. Crystallogr. 66 (2010) 213–221.
[31] S. Xu, B.N. Long, G.H. Boris, A. Chen, S. Ni, M.A. Kennedy, Structural insight into the rearrangement of the switch I region in GTP-bound G12A K-Ras, Acta Crystallogr. D Struct. Biol. 73 (2017) 970–984.